UCRL-JC-132650
PREPRINT

Simulation of Void Growth at High Strain-Rate

J. Belak
R. Minich

This paper was prepared for submittal to the
Materials Research Society Spring Meeting
San Francisco, CA
April 5-9, 1999

December 8, 1998

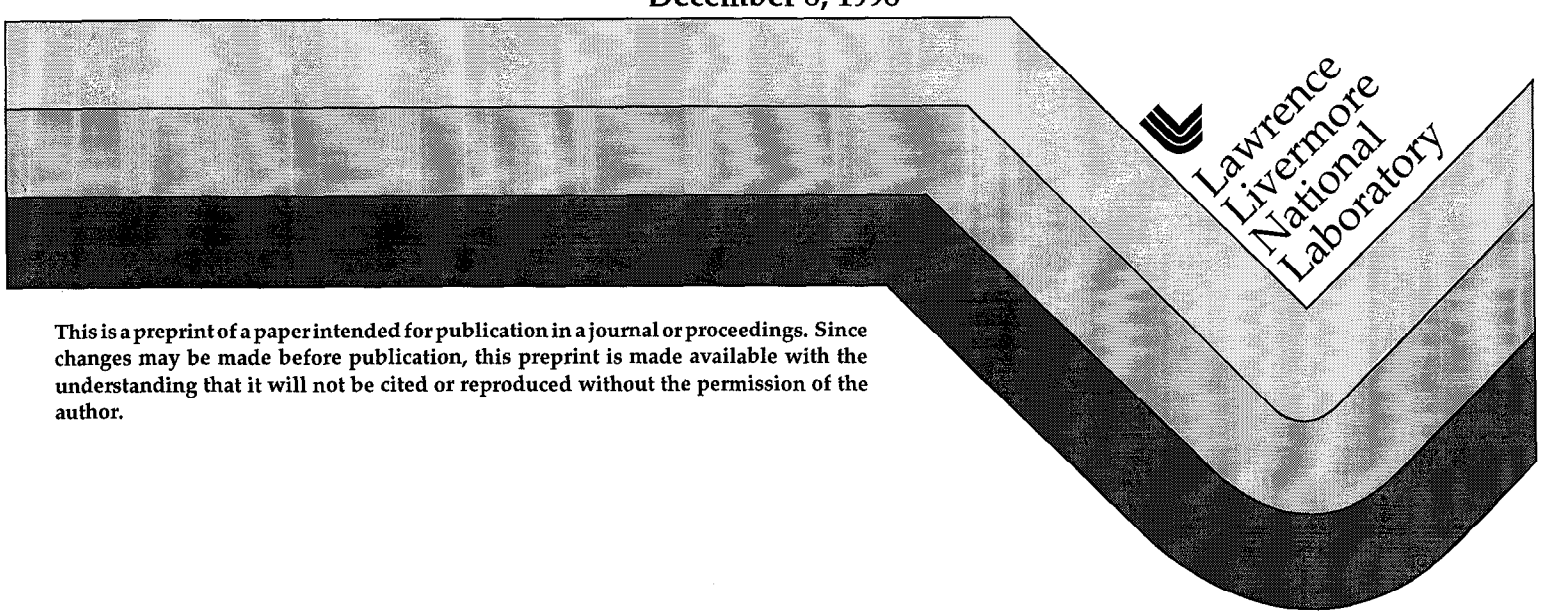

SIMULATION OF VOID GROWTH AT HIGH STRAIN-RATE

J. BELAK and R. MINICH
University of California, Lawrence Livermore National Laboratory, Livermore, CA 95440

ABSTRACT

The dynamic fracture (spallation) of ductile metals is known to initiate through the nucleation and growth of microscopic voids. Here, we apply atomistic molecular dynamics modeling to the early growth of nanoscale (2nm radius) voids in face centered cubic metals using embedded atom potential models. The voids grow through anisotropic dislocation nucleation and emission into a cuboidal shape in agreement with experiment. The mechanism of this nucleation process is presented. The resulting viscous growth exponent at late times is about three times larger than expected from experiment for microscale voids, suggesting either a length scale dependence or a inadequacy of the molecular dynamics model such as the perfect crystal surrounding the void.

INTRODUCTION

The growth of microscopic voids is fundamental to the ductile fracture of metals [1]. Under low strain-rate creep conditions growth is determined by the behavior of vacancies and diffusive processes. An understanding is central to technological problems such as the failure of interconnect lines of microelectronic circuits [2] and the radiation damage of materials in nuclear reactors [3]. At high strain-rates, as occur during shock loading, there is insufficient time for diffusive processes and void growth occurs by plasticity mechanisms. The rich history of experiment [4] and of continuum plasticity models of void growth [1,5-8] has resulted in a highly successful continuum computer code model of failure based on the nucleation and growth of voids [9-11]. However, there remains many unanswered questions concerning the microscopic mechanisms of void nucleation and plastic growth.

In this paper we examine some of these microscopic mechanisms using atomistic molecular dynamics (MD) modeling of the growth of a nanoscale (radius = 2nm) void in copper under high strain-rate isotropic tension.

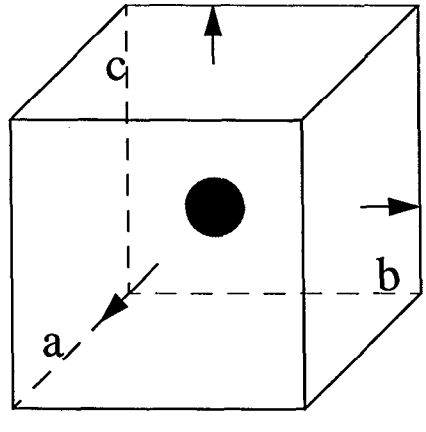

Figure 1. Isotropic tension is simulated by expanding the simulation cell in all directions at a constant rate. A nanoscale void of size R = 2nm $\approx l_{cell}/10$ is cut from the center of the cell.

METHODS

A cubic simulation cell containing N=864000 atoms was created by replicating 60 FCC unit cells along each of the cubic axes. The embedded-atom method [12,13] is used to model copper. The equations of motion are integrated using a Verlet leap-frog algorithm with a time step of 6fs and periodic boundary conditions [14]. The system was simulated at T=300K and P=0 to an equilibrium cell length of l_{cell} = 21.7nm. A void of radius 2nm was then cut from the center of the simulation cell as shown schematically in Figure 1, resulting in a system containing N=860396 atoms. A strain-rate is simulated by rescaling the positions of every atom in the simulation cell as is commonly done in constant pressure MD simulations [15]: $\underset{\sim}{x} = H\underset{\sim}{s}$, where $s \subset [0, 1]$ and $H = \{\underset{\sim}{a}, \underset{\sim}{b}, \underset{\sim}{c}\}$ is a matrix composed of the simulation cell vectors. An isotropic constant strain-rate is simulated by specifying a constant time derivative of H. After equilibrium, the thermostat is turned off and expansion is simulated under adiabatic conditions.

RESULTS and DISCUSSION

The resulting stress averaged over the entire simulation cell is shown in Figure 2 as a function of volume for a strain-rate of $\dot{\varepsilon}=10^9 s^{-1}$. The tension (negative stress) increases monotonically to about 6 GPa after which it turns around and decreases with further expansion. This growth threshold stress agrees well with our previous simulation using comparable voids but smaller overall system sizes [16]. In general larger voids display a smaller growth threshold stress. We stop the simulation when the expanding network of dislocations crosses the periodic boundary.

In a seminal paper on dynamic fracture, Barbee *et.al* [9] measured the growth rate of microscale voids in copper. They observed a viscous growth law of the form:

$$V = V_O e^{\frac{3(\sigma-\sigma_{go})}{4\eta}t} = V_O e^{\alpha t}$$

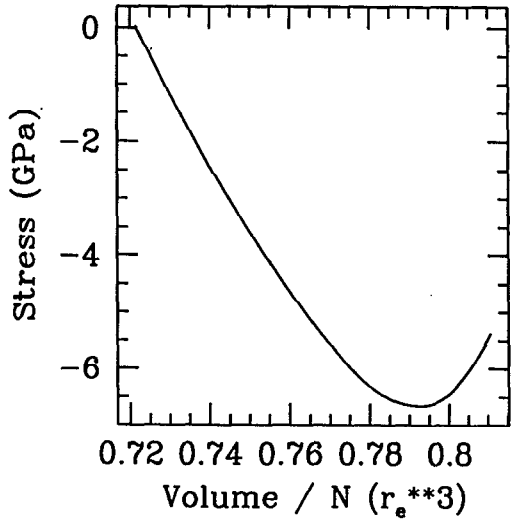

Figure 2. Stress as a function of volume per atom (r_e = 2.54 Å) for isotropic adiabatic expansion of an R=2nm void at $\dot{\varepsilon}=10^9 s^{-1}$.

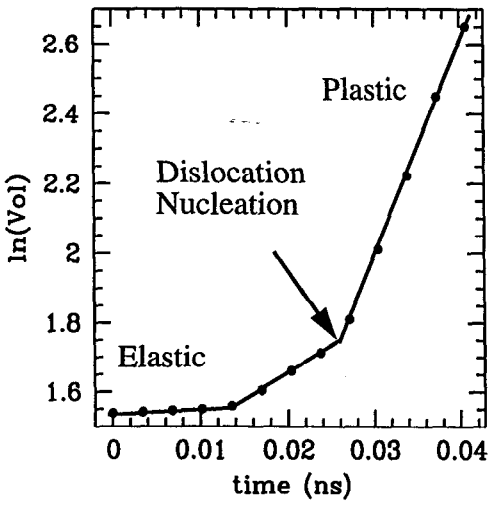

Figure 3. The natural log of the void volume as a function of time for growth of an R=2nm void. The lines are drawn as a guide to the eye.

where V is the void volume, σ is the applied stress, σ_{go} = 0.005 GPa is the growth threshold stress, and η = 0.2 Pa·s is the material viscosity. At an applied stress of 6 GPa (well outside the experimental data), this model predicts a growth exponent of $\alpha \approx 2.2\times10^{10}s^{-1}$.

Comparison with the MD data requires a metric of the void volume within the MD simulation. A void is where the atoms are not. Thus, we define a background grid and compute the sum of unoccupied grid zones. A grid spacing smaller than an atom size leads to spurious results. We find l_{grid} = 0.36nm gives reproducible results consistent with the known initial void radius (2nm). This void volume metric introduces an error which scales as 1/R. We estimate the error to be no more than a few percent for R = 2nm. The resulting volume is shown in Figure 3 as a function of

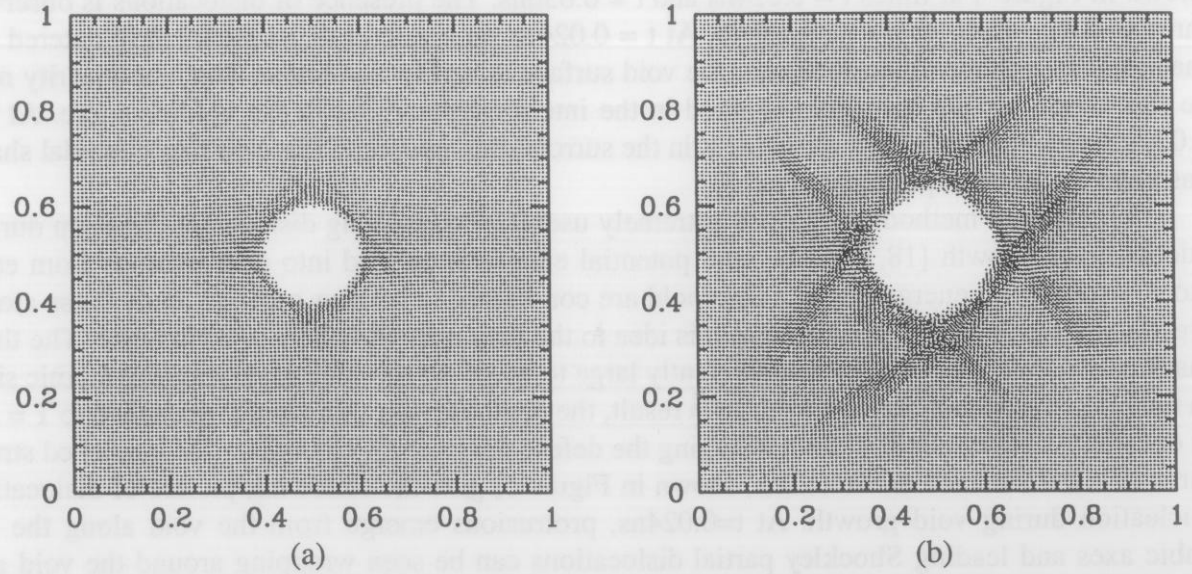

Figure 4. A projection of a thin slice through the center of the simulation cell onto the x-y plane for (a) t=0.024ns and (b) t=0.030ns. The atomic positions are in the unit cube.

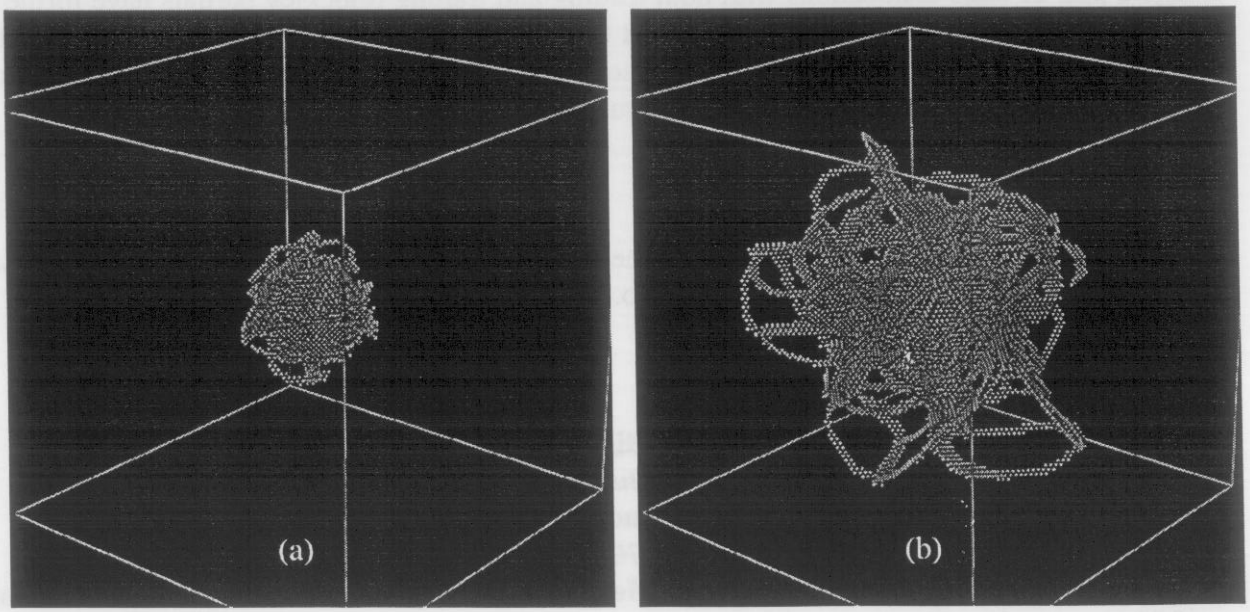

Figure 5. The defect structure at (a) t=0.024ns and (b) t=0.030ns as revealed by the atoms with potential energy 1% above the bulk potential energy at T = 1K.

simulation time. Three distinct, nearly linear regions are observed on the log plot, suggesting exponential growth. Void growth at early time is elastic, displaying no change when normalized by the total system volume. At late time, the growth is fully plastic with a surrounding network of dislocations moving into the material. As shown below, dislocations first emerge from the void surface at $t \approx 0.025$ns and the nature of the intermediate region is not clear. From the slope of the curve at late time we estimate the growth exponent in the simulation to be $\alpha \approx 6.2 \times 10^{10} s^{-1}$. The factor of three higher exponent than expected from experiment is most likely due either to the vast difference in length scale between the simulation and experiment or to the surrounding perfect crystal in the MD simulation.

Two methods of visualizing the nucleating dislocations were considered. First, a thin cross-section through the center of the simulation cell was projected onto the x-y plane. The result is shown in Figure 4 at times t = 0.024ns and t = 0.030ns. The presence of dislocations is observed through their effect on the strain field. At t = 0.024ns no apparent dislocations have entered the materials though the strain field near the void surface is highly non-linear. This nonlinearity may be the reason for the behavior observed in the intermediate region in the volume curve. At t = 0.030ns several dislocations are evident in the surrounding material. The resulting cuboidal shape has been observed experimentally [17].

The second method has proved extremely useful in visualizing dislocation emission during ductile crack growth [18,19]. The total potential energy is divided into contributions from each atom. Atoms with energy above a threshold are considered to be near a defect. Only these atoms are visualized. A naive application of this idea to the data presented here yielded noise. The thermal fluctuations at T = 300K are sufficiently large to wash out the difference between atomic sites in the bulk crystal and near a defect. As a result, the configuration was rapidly quenched to T = 1K at constant volume, hopefully not changing the defect structure significantly. The quenched structures at t=0.024ns and at t=0.030ns, shown in Figure 5, give the following picture of dislocation nucleation during void growth. At t=0.024ns, protrusions emerge from the void along the six cubic axes and leading Shockley partial dislocations can be seen wrapping around the void and terminating on neighboring protrusions. The same image at t=0.021ns shows only the void surface atoms. At t=0.030ns, the dislocation structure is far richer. For example, towards the bottom of the image a pair of edge dislocations with both leading and trailing Shockley partials have formed a junction. This junction, presumable created at the above mentioned protrusions, moves with the dislocation pair away from the void. The process repeats as additional dislocations emerge from the void surface and form even richer microstructures.

ACKNOWLEDGMENTS

Work performed under the auspices of the U.S. Department of Energy by the Lawrence Livermore National Laboratory under contract No. W-7405-ENG-48.

REFERENCES

1. A.S Argon ed., **Topics in Fracture and Fatigue**, Springer-Verlag, New York, 1992.
2. A.F. Bower and D. Craft, *Fatigue and Fracture on Eng. Mater. and Struct.* **21**, 611 (1998).
3. D.R. Olander, **Fundamental Aspects of Nuclear Reactor Fuel Elements**, ERDA (DOE) Technical Information Center, Oak Ridge, 1976.
4. J.S. Rinehart and J. Pearson, **Behavior of Metals Under Impulsive Loads**, ASME, Cleveland, 1954 (reprinted by Dover, New York, 1965).
5. F.A. McClintok, *J. Appl. Mech.* **35**, 363 (1968).

6. J.R. Rice and D.M. Tracy, *J. Mech. Phys. Solids* **17**, 201 (1969).
7. A. Needleman, *J. Appl. Mech.* **39**, 964 (1972).
8. A.L. Gurson, *J. Eng. Mater. Tech.* **99**, 2 (1977).
9. T.W. Barbee, Jr., L. Seaman, R. Crewdson, and D. Curran, *J. Materials* **7**, 393 (1972).
10. D.R. Curan, L. Seaman, and D.A. Shockey, *Phys. Rep.* **147**, 253 (1987).
11. M.A. Meyers and C.T. Aimone, *Prog. Mater. Sci.* **28**, 1 (1983).
12. M.S. Daw and M.I. Baskes, *Phys. Rev. B* **29**, 6443 (1984).
13. D.J. Oh and R.A. Johnson, in **Atomistic Simulation of Materials: Beyond Pair Potentials, V. Vitek and D.J. Srolovitz** eds., Plenum, New York, 1989, p233.
14. M.P. Allen and D.J. Tildesley, **Computer Simulation of Liquids**, Clarendon Press, Oxford, 1987.
15. M. Parrinello and A. Rahman, *J. Appl. Phys* **52**, 7182 (1981).
16. J. Belak, to appear in *J. Computer-Aided Mater. Design* (1998).
17. A.L. Stevens, L. Davison, and W.E. Warren, *J. Appl. Phys.* **43**, 4922 (1972).
18. S.J. Zhou, D.M. Beazley, P.S. Lomdahl, and B.L. Holian, *Phys. Rev. Lett.* **78**, 479 (1997).
19. V. Bulatov, F.F. Abraham, L. Kubin, B. Devincre, and S. Yip, *Nature* **391**, 669 (1998).